

1 **Enhancing cellulose nanofibrillation of eucalyptus Kraft pulp by combining enzymatic and mechanical**
2 **pretreatments**

3 Florencia Cebreiros^a, Santiago Seiler^b, Sai Swaroop Dalli^c, Claudia Lareo^{a,*}, Jack Saddler^c

4 ^aDepartamento de Bioingeniería, Facultad de Ingeniería, Universidad de la República, Julio Herrera y Reissig
5 565, CP 11300, Montevideo, Uruguay.

6 ^bNorman B. Keevil Institute of Mining Engineering, Faculty of Applied Science, University of British
7 Columbia, 517-6350 Stores Road, Vancouver BC V6T 1Z4, Canada.

8 ^cForest Products Biotechnology/Bioenergy Group, Department of Wood Science, Faculty of Forestry,
9 University of British Columbia, 2424 Main Mall, Vancouver BC V6T 1Z4, Canada.

10 *Corresponding author. Tel.: +598 2714 2714 int 18118

11 E-mail address: clareo@fing.edu.uy

12

13 **ABSTRACT**

14 Nanofibrillated cellulose (NFC) extracted from biomass has potential applications in material science and
15 biomedical engineering. In this study, NFC was obtained from bleached eucalyptus Kraft pulp (BEKP) using
16 two commercial enzyme cocktails with cellulolytic and hemicellulolytic activities and non-catalytic protein
17 (swollenin), followed by ultrasonication. This work represents an initial study of the implementation of non-
18 catalytic proteins along with enzymes to extract NFC from biomass. Enzymatic pretreatment was performed to
19 partially remove hemicellulose while enhancing cellulose accessibility for NFC extraction. Cellulase
20 pretreatment with xylanase and swollenin supplementation increased cellulose accessibility and fiber swelling
21 due to extensive hemicellulose removal (>80%) and fiber morphology changes. Subsequent ultrasonication was
22 performed for cellulose nanofibrillation resulting in high NFC yields (61-97%), while keeping NFC properties
23 almost unchanged. Through this process, cellulose nanofibers with diameters ranging from 3 nm to 10 nm were
24 effectively isolated from BEKP, which allows to produce high quality NFC for further applications.

25

26 **Keywords:** nanofibrillated cellulose, enzymatic pretreatment, xylanase, swollenin, ultrasonication

27

28 **1. Introduction**

29 Cellulose-based materials have great potential to replace petroleum-based material in technological
30 applications due to its abundance, biodegradability, and outstanding mechanical properties. The production of
31 cellulose nanomaterials has gained increasing attention over the past few decades due to their potential
32 applications such as aerogel and hydrogel, reinforcement in nanocomposites, packaging materials, and
33 biomedical materials (Abitbol et al. 2016). Two different kinds of cellulose nanomaterials can be obtained from
34 lignocellulosic biomass based on the size, morphology and extraction method: cellulose nanocrystals or
35 nanocrystalline cellulose (NCC) and cellulose nanofibrils or nanofibrillated cellulose (NFC). Typically, NFCs
36 have long, entangled and flexible fibrils with diameters and lengths ranging from 1-100 nm to 500-2000 nm,
37 respectively, containing both crystalline and amorphous cellulose regions (Debiagi et al. 2020; Phanthong et al.
38 2018).

39 NFCs are typically produced by mechanical pretreatment such as mechanical refining and homogenization,
40 ultrasonication, grinding, microfluidization, ball milling (Abdul Khalil et al. 2014; Pires et al. 2019). All these
41 pretreatments operate under high shear force, resulting in the cleavage of cellulose fibers and fibrillation.
42 However, high energy consumptions associated to the process (20,000-30,000 kWh/ton) and product
43 heterogeneity after mechanical treatments are still limiting its implementation (Rajinipriya et al. 2018). To
44 overcome this, combinations of chemicals and/or enzymatic pretreatments are being proposed to facilitate
45 mechanical pretreatments by opening up the starting cellulosic material and further enhancing cellulose
46 accessibility. Thus, the introduction of a chemical or enzymatic pretreatment could facilitate further mechanical
47 pretreatment of microfibrils and bring down the energy consumption up to 20 times (e.g. 1,000 kWh/ton)
48 (Arantes et al. 2020; Rajinipriya et al. 2018; Ramakrishnan et al. 2019). Several chemical pretreatments (e.g.
49 TEMPO-oxidation, carboxymethylation, sulfonation) have been successful in achieving this goal, but there are
50 still many drawbacks associated to process efficiency, use of hazardous reagents and chemical recovery that
51 limits their application (Pires et al. 2019; Ramakrishnan et al. 2019).

52 Enzymatic pretreatment represents an environmentally friendly alternative to chemical pretreatment for
53 NFC production due to high enzyme specificity and less harmful reaction conditions (Michelin et al. 2020;
54 Ribeiro et al. 2019). The use of enzymes during enzymatic pretreatment catalyze the hydrolysis of cellulose
55 fibers and makes fiber fibrillation by following mechanical homogenization much easier. Most of the reported
56 work on nanocellulose production through enzymatic pretreatment were focused mainly on the use of cellulase

57 enzymes, such as endoglucanases (Arantes et al. 2020; Di Giorgio et al. 2020; Long et al. 2017; Ribeiro et al.
58 2019). Endoglucanases are the type of enzymes with the highest interest for the production of nanocellulose,
59 because they break the cellulose polymer into smaller length polymers by acting on the amorphous, or less
60 organized, part of the cellulose. Although enzymatic pretreatment using endoglucanases has shown to be
61 promising for cellulose nanofibrillation enhancement, its efficacy is still limited (Long et al. 2017). However,
62 it has been shown a high degree of synergism between exoglucanases and endoglucanases, which could enhance
63 cellulose hydrolysis and further nanofibrillation (Yarbrough et al. 2017). Additionally, it was recently
64 demonstrated that exoglucanases can hydrolyze microcrystalline cellulose by peeling the cellulose chains from
65 the microcrystalline structure (Merklein et al. 2016). Recently, it was found that the combination of cellulolytic
66 enzymes (cellulases) with cellulase accessory enzymes such as hemicellulases (e.g. xylanases), laccases, and
67 lytic polysaccharide monooxygenases (LPMO) could improve cellulose accessibility during biomass
68 deconstruction, without directly hydrolyzing cellulose (Hu et al. 2018; Zhou et al. 2019). For instance, it was
69 shown that the synergism between cellulases and xylanases increases cellulose hydrolysis efficiency by
70 improving cellulose accessibility, not only due to xylan removal but also to changes in fiber morphology such
71 as increasing fiber porosity and fiber swelling (Long et al. 2017). Even though several studies have been
72 conducted in the past years to produce nanocellulose from different cellulosic substrates through an enzyme-
73 mediated pretreatment, the selection of an effective and low-cost enzyme cocktail still remains a challenge.

74 Moreover, it has been reported that some non-catalytic proteins (CBM, swollenin) enhances the
75 cellulolytic/hemicellulolytic activity by their effects on the dispersion of the cellulose microfibrils and loosening
76 of the cellulose macrofibrils, causing a decrease in cellulose crystallinity and increase in cellulose accessibility
77 (Adsul et al. 2020). This type of non-catalytic proteins is generally required at a very low amount and not
78 present in base enzyme preparations. Swollenin represents one of these types of proteins, which was first
79 isolated and characterized from the cellulolytic fungus *Trichoderma reesei*. Swollenin has been shown to
80 facilitate delamination or fibrillation of substrates, or splitting of microfibrils, resulting in a greater exposure of
81 new crystalline regions of cellulose without producing detectable amounts of reducing sugars (Gourlay et al.
82 2012; Saloheimo et al. 2002). Recently, studies on the supplementation of fungal swollenin into a cellulolytic
83 enzyme preparation for improving enzymatic hydrolysis showed an increase in both cellulose and xylan
84 hydrolysis of lignocellulosic pretreated substrates such as corn stover (Gourlay et al. 2013; Morrison et al.

85 2016). It was suggested that the enhancement on the enzymatic hydrolysis could be due to the opening up of
86 the cellulosic substrate by weakening and/or disrupting of hydrogen bonds within the biomass, which enhanced
87 the enzyme access to the carbohydrates. Moreover, it has been shown that swollenin could promote fiber
88 fragmentation without the presence of non-cellulosic polymers (lignin and hemicellulose) such as dissolving
89 pulps (Gourlay et al. 2013). However, to the best of the authors' knowledge, there are no previous studies on
90 swollenin supplementation into enzyme cocktails for cellulose enzymatic pretreatment to enhance cellulose
91 nanofibrillation.

92 Ultrasonication, which consists on the exposure of the suspension to ultrasonic waves, is one of the
93 mechanical pretreatments used to produce NFC and it was shown to be very effective for cellulose
94 depolymerization (Mahardika et al. 2018). During the ultrasonication process, highly intensive waves are
95 produced by the formation, expansion, and implosion of microscopic gas bubbles when ultrasonic energy is
96 absorbed by molecules, creating hydrodynamic forces that are used for cellulose nanofibers liberation from the
97 material (Abdul et al. 2014). Process optimization using ultrasonication for cellulose fibrillation has previously
98 been reported (Wang and Cheng 2009). Mainly, the effect of temperature, suspension concentration, sonication
99 power and time on fibrillation efficiency was evaluated. However, these conditions greatly depend on the type
100 of cellulosic material used, for example, suspension concentration depends on the size of the fibers, since longer
101 size fiber needs to be treated at lower concentrations. On the other hand, few studies have been reported on
102 combined enzymatic and ultrasonication pretreatment for NFC production. Filson et al. (2009) obtained
103 cellulose nanofibers from recycled pulp using enzymatic pretreatment followed by sonication. Tsukamoto et al.
104 (2013) proposed a method to isolate NFC from enzymatic hydrolysis residues of citrus processing waste using
105 an ultrasonic processor. De Campos et al. (2013) produced NFC from dewaxed and bleached curauá and
106 sugarcane bagasse using enzymes under different enzymatic pretreatment conditions, followed by sonication.

107 In this work, the potential of using commercial enzyme complex and non-catalytic protein during the
108 enzymatic pretreatment process for NFC production to facilitate cellulose nanofibrillation was assessed.
109 Bleached eucalyptus Kraft pulp (BEKP) was used as raw material due to its low cost and abundance. The BEKP
110 was industrially obtained by treating eucalyptus wood chips through the Kraft process, followed by a bleaching
111 process performed in a series of stages involving bleaching agents (chlorine dioxide, hydrogen peroxide and
112 oxygen) and alkaline extractions. One of the main advantages of eucalyptus pulp compared to other cellulosic

113 materials is the shorter fibers, which could facilitate disintegration and reduce energy input. However, it
114 contains considerable amount of hemicellulose (15-20%) which could have a negative effect on cellulose
115 accessibility towards the enzymes, given that it is located on the outer surface and interfibrillar space of
116 cellulose fibers. Thus, removal of hemicellulose from cellulosic biomass could be crucial to produce NFC, since
117 it might be able to enhance opening up the biomass structure and facilitate cellulose nanofibrillation. The aim
118 of this work was to investigate the enzymatic pretreatment consisting of xylanases as hemicellulolytic enzymes
119 and swollenin as non-catalytic protein with commercial cellulase complex to produce NFC from BEKP,
120 followed by an ultrasonication step. This work represents an initial study of the implementation of non-catalytic
121 proteins along with enzymes for NFC production from biomass. The obtained materials were characterized
122 according to their chemical composition, size distribution, fiber swelling, cellulose accessibility, degree of
123 polymerization, crystallinity and thermal stability. NFC yields were calculated as an evaluation of the effects
124 of the different enzymatic pretreatment conditions on the cellulose nanofibrillation.

125

126 **2. Materials and Methods**

127 *2.1. Materials*

128 Bleached eucalyptus Kraft pulp (BEKP) was used as raw material for the production of NFC, which was
129 provided by a commercial local pulp mill (UPM Fray Bentos, Uruguay). The enzymes used in this study were
130 Cellic CTec3 cellulase (279 mg/mL protein content) and HTec xylanase (53 mg/mL protein content) supplied
131 by Novozymes (Davis California). Swollenin, expressed in *Trichoderma reesei*, was used as non-catalytic
132 protein, which was provided by VTT Technical Research Center of Finland and produced as previously
133 described (Gourlay et al. 2013).

134 *2.2. BEKP chemical composition*

135 BEKP was analyzed according to the klason protocol from the TAPPI standard method T222. Sugars were
136 determined by a Dionex ICS-3000 HPLC (Sunnyvale, CA) equipped with an anion exchange column (Dionex
137 CarboPac PA1). Acid soluble lignin was determined by measuring absorbance at 205 nm using Cary 60 UV-
138 Vis spectrophotometer. Glucan, xylan, and lignin contents of BEKP were $77.3 \pm 0.6\%$, $17.6 \pm 0.1\%$ and
139 0.7 ± 0.1 , respectively.

140 2.3. *Enzymatic hydrolysis of BEKP*

141 The enzymatic hydrolysis of BEKP was performed in duplicate at 50°C and 200 rpm in acetate buffer
142 (50 mM, pH 4.8) using CTec3 and HTec accordingly. Before enzyme addition, the slurries were equilibrated at
143 50°C and 200 rpm for 1 h in an orbital shaker (MaxQ 4000, Barnstead/Lab-Line) for pulp disintegration.
144 Enzymatic hydrolysis was carried out at a solid concentration of 2-8% (w/w) and an enzyme loading of 1-
145 7 mg_{protein}/g_{dry pulp}. Samples were taken during hydrolysis and heated at 100°C for 10 min to deactivate the
146 enzyme. Samples were then centrifuged (5,000 rpm for 15 min) to separate the liquid fraction for sugar release
147 analysis, and the residual solid fibers were washed three times with distilled water by centrifugation (5,000 rpm
148 for 15 min). The effects of swollenin on enzymatic pretreatment were evaluated by adding the same amount of
149 swollenin as enzyme loading on protein basis when corresponded. Liquid fractions from the enzymatic
150 hydrolysis experiments were analyzed following NREL protocol (Sluiter et al. 2006), and monomeric sugars
151 were measured by a Dionex ICS-3000 HPLC (Sunnyvale, CA) equipped with an anion exchange column
152 (Dionex CarboPac PA1).

153 2.4. *Ultrasonication*

154 The enzyme-treated BEKP samples were redispersed in deionized water to reach solid consistencies of
155 0.07 to 0.5%. The resulting suspensions were subjected to ultrasonication (50-90% amplitude) with a Q700
156 sonicator (QSonica, Newtown, CT, USA) operating at 20-25 kHz frequency and equipped with a 0.5 inch flat
157 tipped titanium probe. The suspensions were cooled in an ice bath during ultrasonication to avoid overheating,
158 and temperature was kept below 30°C. The ultrasonication was performed with 5 s pulse-on time followed by
159 5 s of pulse-off time for 60 and 120 min when corresponded. The resulting preparations were centrifuged
160 (5,000 rpm for 30 min) in order to separate the micro/nanofibrils.

161 2.5. *NFC yield*

162 Ultrasonicated suspensions were centrifuged at 5,000 rpm for 30 min to separate the nanofibrillated
163 material (in supernatant fraction) from the unfibrillated or partially fibrillated ones, which settle down. The
164 supernatant fraction was then dried to a constant weight at 105°C. The NFC yield was calculated from the
165 following equation:

166
$$NFC\ yield\ (\%) = \frac{M_{NFC} \cdot M_T}{M_{sample} \cdot M_F} \times 100 \quad (1)$$

167 where M_{NFC} denotes the mass of the dried NFC in the supernatant sample; M_T denotes the total mass of the
168 ultrasonicated suspension; M_{sample} denotes the mass of the supernatant sample; M_F denotes the mass (oven-
169 dry basis) of the pulp before ultrasonication.

170 2.6. Analytical methods

171 2.6.1. Water retention value

172 The water retention value (WRV) was measured in duplicate using the TAPPI Useful Method-256.
173 Briefly, 0.5 g (oven-dry basis) of the pulp was soaked in 50 mL of water overnight prior to filtration through a
174 200-mesh screen. The resulting pulp pad was centrifuged at 900 g for 30 min, and finally oven-dried at 105°C
175 overnight. WRV represents the percentage of retained water of the dried substrate, according to the following
176 equation:

$$177 \quad WRV = \frac{W_w - W_d}{W_d} \quad (2)$$

178 where W_w and W_d denote the weight of the wet sample after centrifugation and the dried pulp, respectively.

179 2.6.2. Simons' staining

180 The cellulose accessibility was assessed using Direct Blue (DB) as dye following a modified version
181 of the Simons' staining procedure (Chandra et al. 2008). Briefly, 10 mg (oven-dry basis) of substrates were
182 mixed with 1 M phosphate buffered saline solution (PBS, pH 6) and increasing DB dye concentrations in 1.5-
183 mL screw cap centrifuge tubes. The tubes were incubated overnight at 70°C in an orbital shaker at 180 rpm.
184 After incubation, the tubes were centrifuged at 5,000 rpm for 10 min and the absorbance of the supernatant was
185 read at 455 nm on a Cary 60 UV-Vis spectrophotometer.

186 2.6.3. Degree of polymerization

187 The degree of polymerization (DP) of BEKP and enzyme-treated BEKP was determined by viscosity
188 (25°C) of fiber solution in 0.5 M cupriethylenediamine (CED) solution using Ubbelohde viscometer according
189 to TAPPI standard method T230. The DP was determined using the following equation (Immergut et al. 1953;
190 Hamad and Hu 2010):

$$191 \quad DP^{0.905} = 0.75[\eta] \quad (3)$$

192 where η denotes the intrinsic viscosity expressed in cm³/g and calculated according to ASTM D1795-13.

193 2.6.4. *X-ray diffraction (XRD)*

194 BEKP and enzyme-treated BEKP were analyzed using X-ray diffractometer (MiniFlex600, Rigaku).
195 The samples were dried and ground into powders for XRD test. The diffracted intensity of CuK_α radiation
196 (40 kV and 15 mA) was measured in a 2θ range between 5° to 60° with increments of 0.05° , at a scanning rate
197 of $4^\circ/\text{min}$. The relative crystallinity index (CrI) was calculated using the Segal et al. (1959) method, as the
198 difference between the maximum intensity of the peak located at $2\theta = 22^\circ\text{-}23^\circ$, and the minimum intensity
199 located between the major peaks at $2\theta = 18^\circ\text{-}19^\circ$ divided by the intensity of the highest peak.

200 2.6.5. *Transmittance of NFC suspensions*

201 The light transmittance of NFC suspensions (0.1% w/v) from BEKP and enzyme-treated BEKP was
202 measured in the range of 400 nm to 800 nm using Cary 60 UV-Vis spectrophotometer.

203 2.6.6. *Thermogravimetric analysis (TGA)*

204 The thermal stability of BEKP, enzyme-treated BEKP and NFC was studied using thermogravimetric
205 analysis (TGA) and derivative thermogravimetric analysis (DTG) with a thermogravimetric analyzer
206 (TGA 4000, PerkinElmer, USA). The samples were analyzed under a nitrogen atmosphere with a gas flow of
207 20 mL/min by heating the material from 35°C to 600°C at a heating rate of $10^\circ\text{C}/\text{min}$.

208 2.6.7. *Morphological analysis - AFM*

209 The morphology of the NFCs was studied by atomic force microscopy (AFM) using Multimode AFM
210 Nanoscope-III from Veeco Instruments (Santa Barbara, CA, USA) with the PeakForce tapping mode. A freshly
211 cleaved mica was chemically modified with a cationic compound (3-aminopropyl)triethoxysilane (APTES)
212 according to previous studies (Aissa et al. 2019). Briefly, a drop of 0.1% w/v of APTES solution was placed on
213 a cleaved mica surface for 30 s and then thoroughly rinsed with nanopure water. The samples were prepared by
214 depositing a drop of diluted NFC suspension (0.01% wt) on the modified mica surface and leaving it to dry for
215 at least 1 h. AFM images were taken at a scan rate of 0.7 Hz using a RTESPA-150 cantilever probes with a
216 nominal spring constant of 7 N/m. AFM images were analyzed using NanoScope Software 8.10 (Veeco, Santa
217 Barbara, CA, USA).

218 2.6.8. *Fiber Quality Analysis (FQA)*

219 Fiber dimensions and fines content of BEKP and enzyme-treated BEKP were determined using a Hi-
220 Resolution fiber quality analyzer (LDA02-series, OpTest Equipment Inc, Hawkesbury, Canada). About 10,000
221 fibers were collected to calculate the fiber length distribution in the range of 0.07 mm to 10.0 mm. Fines were
222 defined as fiber lengths between 0.07 mm to 0.20 mm.

223 2.6.9. *Dynamic Light Scattering (DLS)*

224 The size distribution of enzyme-treated BEKP suspensions was also evaluated with a Malvern Mastersizer
225 Hydro 2000G/S (Malvern Instruments Limited, Worcestershire, UK). The samples were suspended in water
226 and analyzed with the particle size analyzer using dynamic light scattering (DSL).

227

228 3. Results and discussion

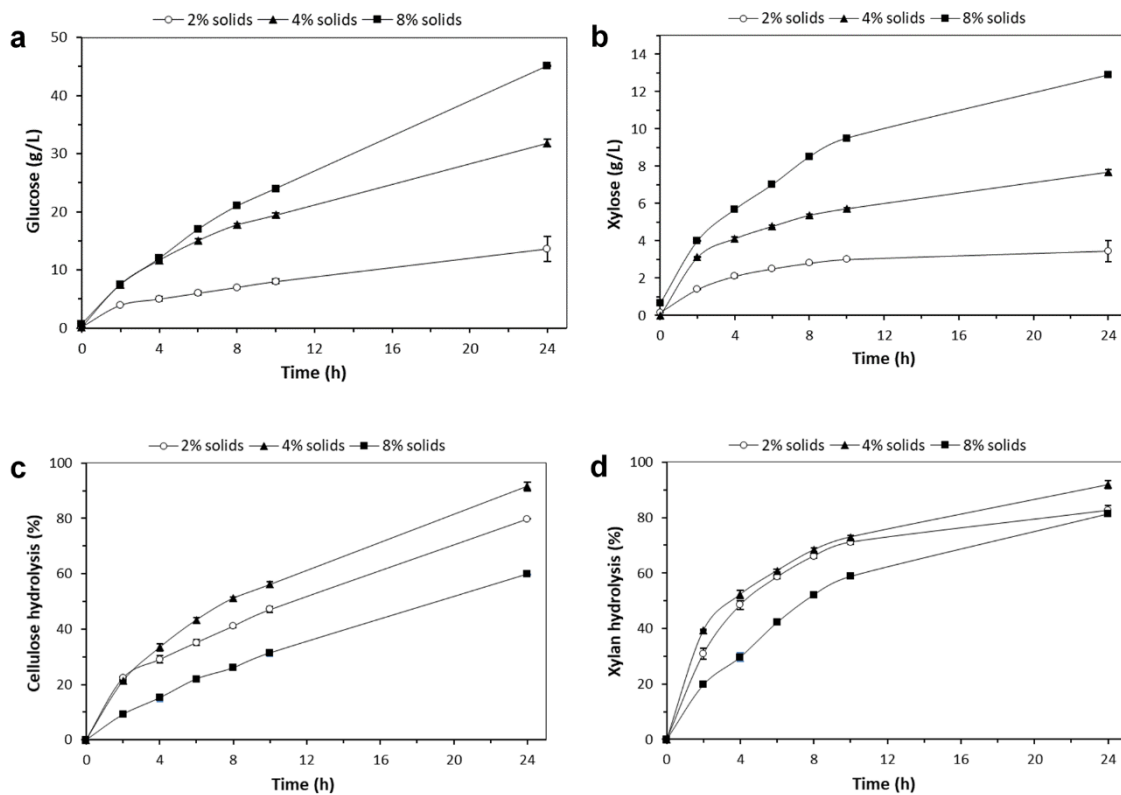
229 3.1. *Enzymatic pretreatment of eucalyptus Kraft pulp: effect of cellulase, xylanase and swollenin* 230 *preparation*

231 In this study, a commercial BEKP was used as raw material to produce NFC using a combination of
232 enzymatic and mechanical pretreatment. Enzymatic pretreatment was performed using enzyme cocktails
233 (cellulase, xylanase) and non-catalytic protein (swollenin) to evaluate the partial removal of hemicellulose from
234 BEKP and catalyze the hydrolysis of cellulose fibers to enhance cellulose accessibility and make fibrillation
235 easier. Enzymatic hydrolysis experiments of BEKP were initially carried out for 24 h using CTec3 and varying
236 the solids loading (2, 4 and 8% w/v) (Figure 1). Low and relatively high solids loading was selected in this
237 study to evaluate possible effects due to mass transfer limitations and the recovery of released sugars at an
238 increased concentration. As it was expected, higher glucose and xylose concentrations were obtained with
239 increasing solids loading, reaching 45 g/L and 13 g/L, respectively, for 8% solids loading.

240 However, similar glucose and xylose concentrations were obtained during the first 4 h of hydrolysis
241 when the solids loading was increased from 4% to 8%, indicating similar enzymatic hydrolysis rates. This
242 suggests possible mass transfer limitations at the initial stages of hydrolysis due to the higher solids content. In
243 order to determine if mass transfer or other limitations affected the hydrolysis performance, results were
244 analyzed in terms of cellulose and xylan hydrolysis (Figure 1b). It can be observed that higher cellulose (33%)
245 and xylan (52%) hydrolysis was reached at 4% solids loading, but further increasing solids loading up to 8%

246 w/v negatively affected the hydrolysis rates (15% and 30% for cellulose and xylan hydrolysis, respectively).
 247 Similar results in terms of hydrolysis rates were observed when the solids loading decreased to 2% (29% and
 248 49% for cellulose and xylan hydrolysis, respectively) compared to 4% during the first 4 h of hydrolysis.
 249 However, lower glucose (5.0 g/L) and xylose (2.1 g/L) concentrations were reached in this case. Consequently,
 250 considering that after 24 h of hydrolysis significant cellulose degradation was achieved due to glucose release,
 251 further enzymatic hydrolysis experiments were performed at 4% solids loading for 4 h that minimizes cellulose
 252 loss and increases the released glucose (11.7 g/L) and xylose (4.1 g/L) concentrations. However, cellulase
 253 pretreatment of BEKP resulted in relatively low hemicellulose removal, considering that only 50% of the
 254 original xylan was effectively removed.

255



256

257 **Fig 1.** (a) Glucose, (b) xylose, (c) cellulose hydrolysis and (d) xylan hydrolysis profiles during enzymatic
 258 hydrolysis of BEKP under different solids loading conditions (2%, 4% and 8%).

259

260 Supplemental of hemicellulolytic enzymes (xylanase) and non-catalytic protein (swollenin) to the
 261 cellulase pretreatment of BEKP was performed to enhance xylan removal and thus improve cellulose

262 accessibility. Also, it has been previously demonstrated the synergistic effect between cellulases and xylanases
 263 to open up the cellulose fiber structure in order to enhance further cellulose nanofibrillation (Long et al. 2017).
 264 The enzymatic pretreatment was first evaluated using the commercial xylanase preparation commonly used for
 265 biomass deconstruction (HTec) alone and in combination with CTec3 using BEKP as substrate. The xylanase
 266 was added by replacing a portion of cellulase enzyme with xylanase enzyme (cellulase:xylanase ratios of 1:0,
 267 0:1, 1:1, 2:1, 1:2 on mass basis) to avoid an increase in the total protein loading (Table 1). The highest degree
 268 of synergism between the enzymes was observed at a cellulase:xylanase ratio of 1:1, which resulted in a
 269 substantial increase in both cellulose and xylan hydrolysis (43% cellulose and 76% xylan hydrolysis, Table 1).
 270 In order to limit the amount of cellulose loss during hydrolysis, enzymatic pretreatment was carried out at lower
 271 total protein loading (Table 1). However, decreasing the total protein loading from 4 mg_{protein}/g_{solid} to 3
 272 mg_{protein}/g_{solid} significantly reduced the xylan removal during enzymatic hydrolysis, which could have a negative
 273 effect on enhancing cellulose accessibility.

274

275 **Table 1.** Effect of xylanase and swollenin supplementation to cellulase pretreatment of BEKP on cellulose
 276 and xylan hydrolysis at 4% solids loading after 4 h.

Cellulase:xylanase ratio	Swollenin addition	Total protein loading (mg _{protein} /g _{solid})	Cellulose hydrolysis (%)	Xylan hydrolysis (%)
1:0	No	7.0	33.4 ± 1.3	52.3 ± 1.5
0:1	No	1.4	6.3 ± 0.1	46.8 ± 1.0
2:1	No	5.2	34.2 ± 1.9	54.3 ± 2.1
1:2	No	3.2	30.9 ± 2.2	56.4 ± 2.8
1:1	No	4.2	43.1 ± 0.2	76.2 ± 0.4
1:1	No	3.0	28.5 ± 2.4	49.3 ± 2.2
1:1	No	1.5	19.9 ± 1.6	39.1 ± 1.3
1:1	No	1.0	9.8 ± 0.2	25.8 ± 0.1
1:1	Yes	8.4	46.3 ± 1.6	84.6 ± 2.0

277

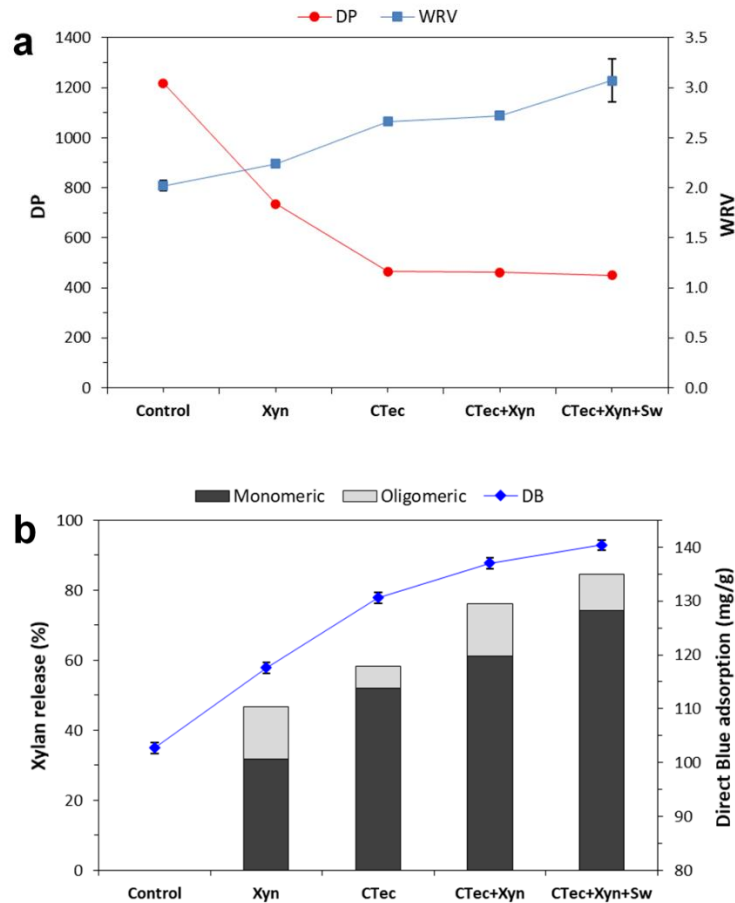
278 On the other hand, swollenin was assessed in this study in combination with xylanase (Table 1), since
279 it has been previously reported by other authors that swollenin has strong synergism with xylan degrading
280 enzymes (Gourlay et al. 2012, 2013). According to the results obtained, swollenin was able to disrupt the
281 relatively loosely ordered xylan structure during cellulase and xylanase enzymatic pretreatment, since an
282 increased xylan hydrolysis (85%) was reached compared to enzymatic pretreatment without swollenin
283 supplementation (76%). Moreover, no increased cellulose hydrolysis (46%) was observed with the use of
284 swollenin, which suggests that swollenin does not cause cellulose degradation but has a significant effect on
285 the hemicellulose component.

286 After enzymatic pretreatment, cellulosic fiber characteristics such as cellulose accessibility (Simon's
287 staining techniques with Direct Blue, DB), fiber swelling (water retention value, WRV) and degree of
288 polymerization (DP) were assessed (Figure 2). The cellulase pretreatment of BEKP has shown to significantly
289 reduce the DP (from 1218 to 465). This was expected considering that cellulases could randomly cleave the
290 glycosidic linkages in both the disorganized (also known as amorphous) and organized (also known as
291 crystalline) regions of the cellulose fiber, which induces the cellulose DP reduction (Reese et al. 1957).
292 Moreover, since xylan plays an important role in protecting cellulose chains against degradation (Gomes et al.
293 2014), xylan removal by cellulase pretreatment may have caused cellulose becomes more susceptible to
294 depolymerization. DP reductions with enzyme pretreatment was also reported by other authors (Djafari
295 Petroudy et al. 2015; Long et al. 2017; Wang et al 2014). On the other hand, even though xylan removal was
296 increased during cellulase and xylanase enzymatic pretreatment, no further DP reduction was observed in this
297 case. The greater exposure of cellulose due to extensive xylan removal could have caused a higher cellulose
298 depolymerization and, thus, lower DP values. On the other hand, considering that xylans are categorized as
299 short chain polysaccharides (Djafari Petroudy et al. 2015), removal of these low molecular weight
300 carbohydrates may lead to an increase in the DP extent (Gomes et al. 2014). This effect may have offset the DP
301 reduction by cellulose depolymerization occurring when xylan is removed and, thus, DP remained almost
302 unchanged. Despite of this, the depolymerization reached could help the formation of NFC by subsequent
303 ultrasonication. On the other hand, xylanase pretreatment of BEKP resulted in lower DP variations (from 1218
304 to 735) compared to cellulase pretreatment (Figure 2a). This was also shown by Zhou et al. (2019) and reflects
305 the difference in the catalytic activity of the enzymes used.

306 The WRV, which can be an indicator of overall fiber accessibility, showed a contrary trend to the
307 observed for DP. Moreover, results showed that the enzymatic pretreatment may have increased the cellulose
308 accessibility, considering the significant increase in the DB adsorption and the WRV observed (Figure 2a and
309 Figure 2b). Even though the supplementation of xylanases to cellulase pretreatment had little effect on the fiber
310 swelling according to the WRV (Figure 2a), the synergism between cellulases and xylanases further improved
311 the cellulose accessibility of enzyme-treated BEKP according to DB adsorption (Figure 2b). The improvement
312 achieved on the cellulose accessibility indicated that the fiber structure was further opened up, which could be
313 beneficial for subsequent cellulose nanofibrillation. The partial replacement of cellulase by xylanase had very
314 little effect on the cellulose DP of the enzyme-treated BEKP obtained (Figure 2a). This indicates that the
315 combination of these enzymes was suitable for keeping cellulose properties while improving cellulose
316 accessibility, without causing further cellulose degradation. On the other hand, the addition of swollenin
317 considerably improved the cellulose accessibility and fiber swelling (Figure 2). It was apparent that the
318 increased xylan hydrolysis could have facilitated the enzyme access to the cellulosic component of BEKP thus
319 opening up the biomass structure and cellulose accessibility. Also, an increased WRV achieved with the use of
320 swollenin might suggest exposure of greater amount of cellulose due to xylan removal that enhanced water
321 retention, since it is likely that xylan acts as a physical barrier possibly coating cellulose microfibrils and/or
322 limiting cellulose fiber swelling. However, it was less able to alter the more highly-ordered cellulose structure,
323 since the degree of polymerization (DP) kept almost unchanged and no significant cellulose degradation
324 occurred (Figure 2a). Results obtained in this work showed how beneficial the addition of xylanases and
325 swollenin to cellulase pretreatment can be in enhancing major fiber characteristics such as fiber swelling and
326 overall cellulose accessibility, which could facilitate downstream cellulose nanofibrillation.

327 Regarding xylan release during enzymatic pretreatment, it should be noted that both cellulase (CTec3)
328 and xylanase (HTec) preparations showed good performance for xylan degradation (Figure 2b), since
329 considerable amounts of xylose (32-74%) and soluble xylooligomers (6-15%) were released from the original
330 xylan present in the BEKP. A higher proportion of xylooligomers than of xylose was released when xylanase
331 was employed alone (32%) and in combination with cellulase (20%) during enzymatic pretreatment, compared
332 to cellulase pretreatment (10%). This suggests that the commercial xylanase preparation used in this study may
333 lack of β -xylosidase activity to further convert xylooligomers to xylose by hydrolysis. However, the use of

334 swollenin in combination with cellulase and xylanase enhanced xylan hydrolysis, while decreasing the
 335 proportion of xylooligomers in the liquid fraction to 12%. This allows to get released sugars in a suitable way
 336 which represents a possible feedstock to produce other value-added chemicals (Bondancia et al. 2017; Pereira
 337 and Arantes, 2020).



338

339

340 **Fig 2.** Characteristics of enzyme-treated BEKP: (a) fiber swelling by water retention value (WRV) and degree
 341 of depolymerization (DP), (b) xylan release in monomeric and oligomeric forms and cellulose accessibility by
 342 Simon's staining with Direct Blue (DB). CTec, Xyn and Sw are assigned to CTec3, HTec and swollenin,
 343 respectively.

344

345 *3.2. Effect of enzymatic pretreatment on pulp fiber properties*

346

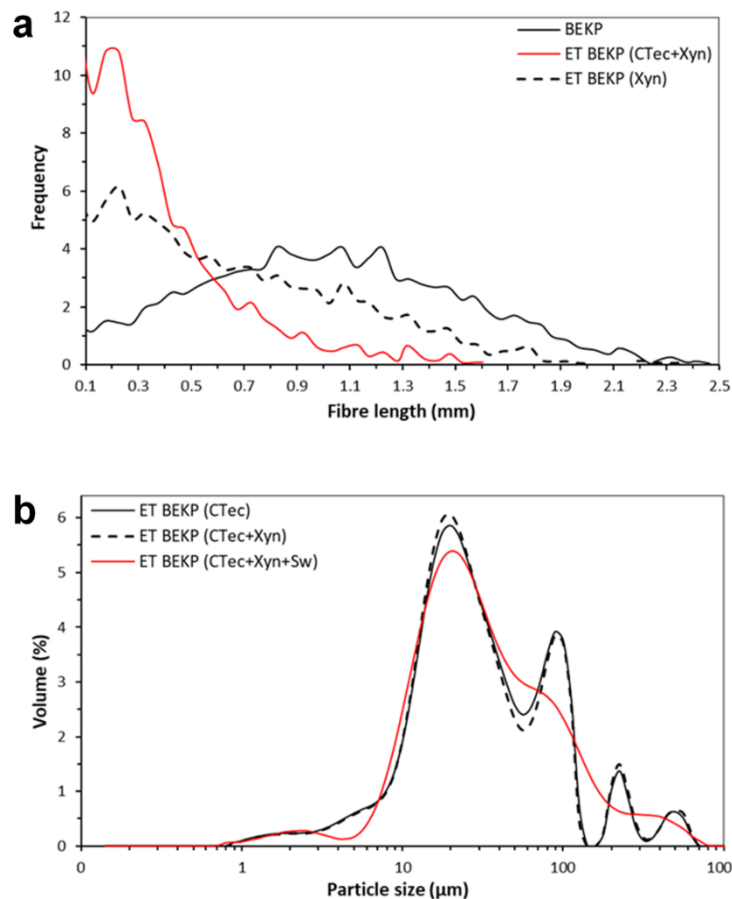
347 Since it has been shown that hemicellulose contributes to fiber strength and its solubilization influences
 pulp fiber properties, fiber dimensions and fiber size distribution of BEKP and enzyme-treated BEKP samples

348 were determined by fiber quality analysis (FQA) (Figure 3a). FQA equipment has been extensively used in the
349 past years for pulp and paper studies to evaluate changes at the fiber level. According to FQA results, BEKP
350 was 15.1 μm in mean width and 1.02 mm in length, containing 25% of fines (fibers with length ranging from
351 0.07 mm to 0.2 mm). After enzymatic pretreatment, significant fiber fragmentation was observed using
352 cellulase alone or in combination with xylanase and swollenin (Figure 3). When xylanase was used alone during
353 enzymatic pretreatment of BEKP, the fiber length decreased up to 0.64 mm, with a fines content of 51%.
354 However, cellulase pretreatment significantly increased the level of fibrillation, as the fines content increased
355 up to 87% and 65% when used alone or in combination with xylanase, respectively. Due to the high fines
356 content of the enzyme-treated BEKP, size distribution after enzymatic pretreatment using cellulase enzyme was
357 determined by dynamic light scattering analysis (DLS) (Figure 3b).

358 Although microscopy analysis (e.g. TEM) could be used to determine size dimension and distribution
359 of samples with high fiber fragmentation, the accuracy of microscopy measurements is limited to the small
360 fraction of sample analysed relative to the whole sample. Because of this, DLS method was used in this study
361 for a more complete evaluation of the size distribution of enzyme-treated BEKP samples. DLS is a well-known
362 method which determined the hydrodynamic “apparent particle size” of cellulose micro/nanomaterials by
363 measuring the scattered light intensity caused by particles undergoing Brownian motion (Yadav et al., 2017;
364 Foster et al., 2018). By assuming that the particles have a single and constant rate of diffusion (e.g. spherical
365 particles), the intensity is related to the particle size by the Stokes-Einstein equation (Foster et al., 2018).
366 However, since rod-like fibers are treated as spherical particles, DLS measurements does not give absolute
367 values for size distribution (Qua et al., 2011). Instead, DLS gives a hydrodynamic “apparent size” distribution
368 that can be used to compare between samples that were prepared under different pretreatment conditions.
369 Several authors used this technique to assess the size distribution of cellulose micro/nanomaterials (Qua et al.,
370 2011; Yadav et al., 2017; Foster et al., 2018; Tibolla et al., 2018; Ramakrishnan et al., 2019; Ferreira et al.,
371 2020).

372 According to DLS results, fibers fractionation was apparent during cellulase pretreatment of BEKP,
373 reaching an average hydrodynamic size of 28.6 μm . However, there were still some large fibers in the range of
374 200-800 μm , which should be fractionated during subsequent ultrasonication. When cellulase was used in
375 combination with xylanase during enzymatic pretreatment, the average hydrodynamic size remained relatively

376 constant (27.8 μm) and no significant changes was observed compared to cellulase pretreatment (Figure 3b).
 377 On the other hand, the addition of swollenin during enzymatic pretreatment allowed to achieve a more uniform
 378 hydrodynamic size distribution of the fibers, without significantly affecting the average hydrodynamic size
 379 (29.8 μm). This may be explained by the increased fiber swelling observed with the use of swollenin during
 380 enzymatic pretreatment, which enhanced fiber fragmentation and, thus, less larger fibers in the range of 60-
 381 800 μm were observed. It should be noted that in all cases between 80 and 90% of the fibers were less than
 382 100 μm size on average, which is in the microfibril range. Also, considerable size reduction after enzymatic
 383 pretreatment of BEKP was reached, which implies that fibers became smaller due to increased degree of
 384 microfibrillation and thus, greater exposure of surface area on the fibrils occurred. This correlates quite well
 385 with the increased WRV of enzyme-treated BEKP samples related to both fibrils and microfibrils surface area.



386

387

388 **Fig 3.** Size distribution of BEKP and enzyme-treated (ET) BEKP samples using (a) fiber quality analysis and
 389 (b) dynamic light scattering. CTec, Xyn and Sw are assigned to CTec3, HTec and swollenin, respectively.

390

391 3.3. NFC production using ultrasonication

392 NFCs were produced by enzymatic pretreatment followed by ultrasonication, being this last step
 393 important for fiber defibrillation in nanofibers by ultrasound hydrodynamic forces. Process conditions such as
 394 suspension consistency, sonication intensity (amplitude) and time were evaluated during ultrasonication of
 395 enzyme-treated BEKP, and results were analyzed in terms of NFC yields (Table 2). NFC yields of 61-93% were
 396 reached for enzyme-treated BEKP, which indicates that cavitation was effective for opening the microfiber
 397 structure, releasing the nanofibrils from the fiber cell wall. Also, relatively high NFC yield (33%) was obtained
 398 from BEKP at the highest ultrasonication intensity, which demonstrates the efficiency of the ultrasonication
 399 process for NFC production from this type of cellulosic material. However, it should be mentioned that
 400 eucalyptus pulp presents shorter fibers compared to other woody materials (e.g. Pinus pulp) which facilitates
 401 disintegration.

402
 403 **Table 2.** NFC yields of different ultrasonication conditions obtained from untreated and enzyme-treated (ET)
 404 BEKP samples.

Substrate	Amplitude (%)	Solid consistency (%)	NFC yield (%)
BEKP	90	0.30	33.1 ± 0.1
ET BEKP (CTec)	50	0.30	61.3 ± 4.4
	70	0.30	74.5 ± 1.4
	90	0.07	78.9 ± 4.9
	90	0.15	92.7 ± 2.0
	90	0.20	93.0 ± 2.7
	90	0.30	92.7 ± 2.0
	90	0.50	77.0 ± 3.0
ET BEKP (CTec+Xyn)	90	0.30	97.3 ± 1.1
ET BEKP (Xyn)	90	0.30	73.0 ± 1.1
ET BEKP (CTec+Xyn+Sw)	90	0.30	95.9 ± 0.2

Ultrasonication pretreatment was performed for 60 min in all cases.

405

406 The yield of NFCs produced was increased from 79% to 93% by increasing solid consistency from
407 0.07% to 0.15%. While increasing the fibers concentration in the suspension, the hitting and crashing effects
408 among the fibers that are accelerated by the microbubbles aquatic force became significant, enhancing the
409 disintegration of the fibers and degree of nanofibrillation. No significant difference was observed in NFC yields
410 when increasing solid consistency up to 0.3%. However, NFC yield was significantly reduced to 77% when the
411 solid consistency was increased up to 0.5%, which suggests that further increasing solid consistencies
412 negatively affect cellulose nanofibrillation. This could be due to poor agitation and inadequate stirring at high
413 solid concentrations by the microbubbles force generated during ultrasonication, so the fibers have a lower
414 chance of passing the probe tip. A similar effect was also reported by Wang and Cheng (2009) with increasing
415 concentrations of cellulose suspensions. Consequently, a solid consistency of 0.3% was selected for further
416 experiments, which allowed to obtain higher concentrations of NFCs in supernatants.

417 Regarding ultrasonication intensity, NFC yield changed greatly depending on the ultrasonication
418 amplitude used (Table 2). Higher the amplitude (90%), higher the NFC yield achieved (93%). When an
419 amplitude of 50% was used during ultrasonication, the NFC yield was only 61%, which increased to 74% by
420 increasing amplitude to 70%. It was demonstrated that higher operating amplitude facilitated cellulose
421 nanofibrillation, which led to almost 100% conversion from microfibers to nanofibers (nanocellulose) in
422 enzyme-treated BEKP samples. Based on the NFC yields determination, the best conditions selected for the
423 ultrasonication process was: 90% ultrasonication amplitude, 60 min process time and 0.3% solid consistency.
424 However, ultrasonication was also performed for 120 min (data not shown), but no NFC yield improvement
425 was achieved for any of the different substrates.

426 Finally, the degree of nanofibrillation was compared among the different enzyme-treated BEKP
427 samples (Table 2). Results showed that the nanofibrillation degree was increased when cellulase pretreatment
428 was supplemented with xylanase enzyme, which allowed to achieve the highest NFC yield after ultrasonication
429 (97%). This correlates quite well with the increased cellulose accessibility and fiber swelling of the substrates
430 (Figure 2). No significant difference in cellulose nanofibrillation was observed with the addition of swollenin
431 during enzymatic pretreatment, which also allowed to achieve almost complete conversion of microfibers to
432 nanofibers (96%). This was expected due to the increased cellulose accessibility and fiber swelling observed
433 for this enzyme-treated sample, which was previously discussed. Moreover, these results demonstrated that the

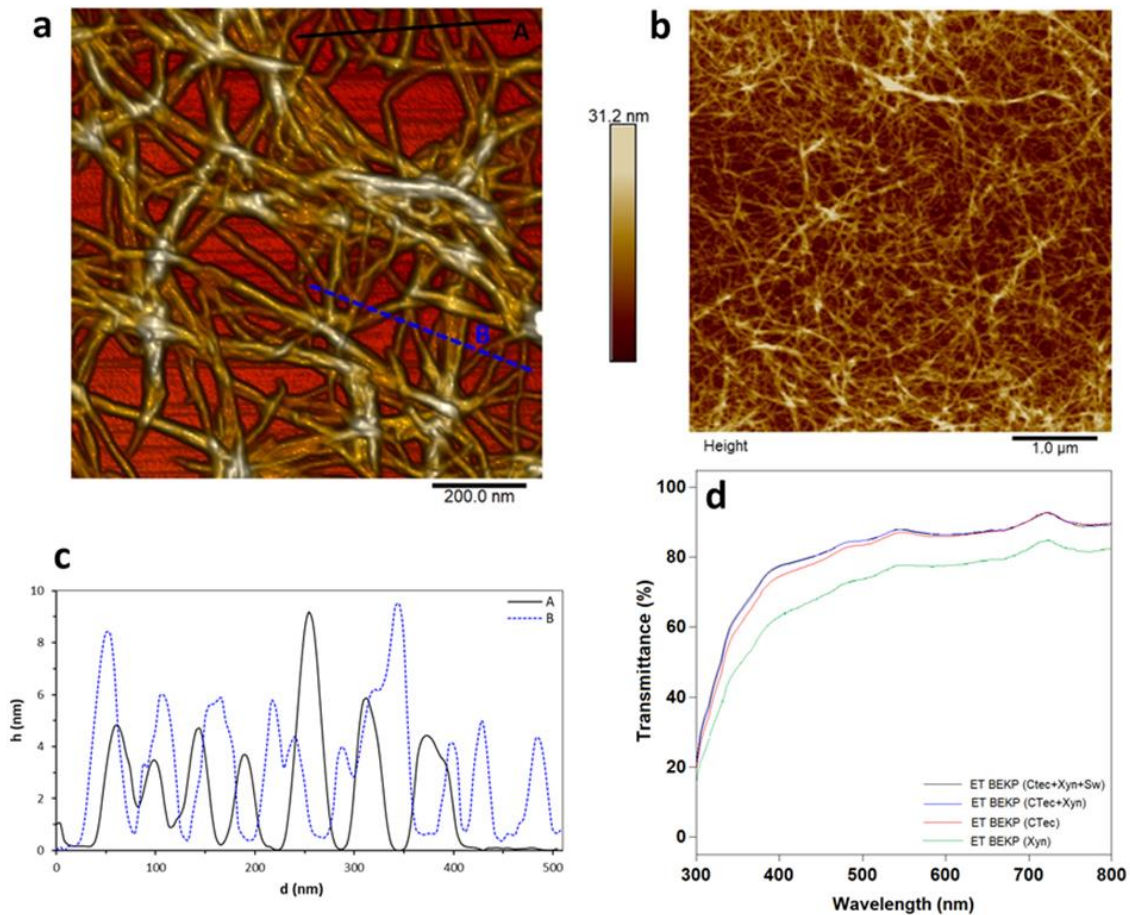
434 xylan removal achieved using swollenin during enzymatic pretreatment facilitated the initial fibrillation to
435 separate cellulose fibrils, but had no significant effect on nanofibrillation through subsequent ultrasonication.
436 However, it should be noted that, despite the extensive xylan removal under this condition (85%), no negative
437 effect was observed on cellulose nanofibrillation in this study.

438 On the other hand, lower cellulose nanofibrillation was obtained using enzyme-treated BEKP with
439 xylanase alone (73%), probably due to the lower cellulose accessibility of the substrate after enzymatic
440 pretreatment. Nevertheless, this cellulose nanofibrillation degree resulted higher than the BEKP nanofibrillation
441 (33%), which demonstrates that enzymatic pretreatment, using cellulases and/or xylanases, effectively
442 enhanced cellulose nanofibrillation during the ultrasonication process.

443

444 *3.4. Morphology and size of NFCs*

445 The morphology of the NFCs prepared through enzymatic and ultrasonication pretreatment was
446 analyzed by AFM observations (Figure 4a and Figure 4b). For all samples, observations revealed networked
447 and ribbonlike NFC samples, with a quite uniform size distribution. Though the fibers were entangled by the
448 long lengths, they were well dispersed into almost elementary fibril levels. The diameter of the nanofibrils was
449 estimated from the height profile and resulted in the range of 3-10 nm for individual non-aggregated nanofibrils
450 (Figure 4c). This indicates efficient fibrillation and separation of NFC through the combination of enzymatic
451 and mechanical pretreatment. Long et al. (2017) also produced NFCs from BEKP by endoglucanase
452 pretreatment followed by ultrasonication. However, the diameters of NFCs obtained in this study (3-10 nm)
453 were smaller than the nanocellulose products reported in their study (about 50-150 nm), which indicates
454 improved cellulose nanofibrillation. Also, Baati et al. (2017) reported NFC production with a fiber size in the
455 range of 2-5 nm after using a twin-screw extruder for fibers disintegration, which were chemically pretreated
456 (TEMPO-Mediated oxidation) prior to mechanical pretreatment. In their study, smaller NFC sizes were mainly
457 due to the stronger pretreatment which facilitated cellulose disintegration and further nanofibrillation, with a
458 quite uniform width distribution.



459

460 **Fig 4.** (a,b) AFM images of NFCs produced after ultrasonication of enzyme-treated BEKP, (c) cross-section
 461 profile analysis (the arrows (A, B) mark the points used for height measurements) and (d) UV-Vis transmittance
 462 spectra of NFC suspensions (0.1% w/v approx.). CTec, Xyn and Sw are assigned to CTec3, HTec and swollenin,
 463 respectively.

464

465 Recently, turbidity measured as the amount of light transmitted has been proposed as a quick method
 466 to assess the dispersion of cellulose nanomaterials (Foster et al. 2018). Thus, lower turbidity of suspensions
 467 means more fibrillated NFCs. Light transmittance was determined by spectrometry to evaluate the opacity and
 468 ensure uniform nanofibrils morphology of NFC suspensions (Figure 4d). Transmittance values of over 80% at
 469 500 nm demonstrates NFC suspensions well dispersed in water and with nano-properties. As expected, the use
 470 of xylanase enzymes and swollenin during cellulase pretreatment improved the transparency of NFC
 471 suspensions after ultrasonication (82-84% at 500 nm), which demonstrates an improved cellulose

472 nanofibrillation. However, lower transparency values (73% at 500 nm) were obtained by using xylanase
473 enzymes alone during enzymatic pretreatment, which suggests lower cellulose nanofibrillation degree. These
474 results correlate quite well with the NFC yields previously discussed (Table 2).

475

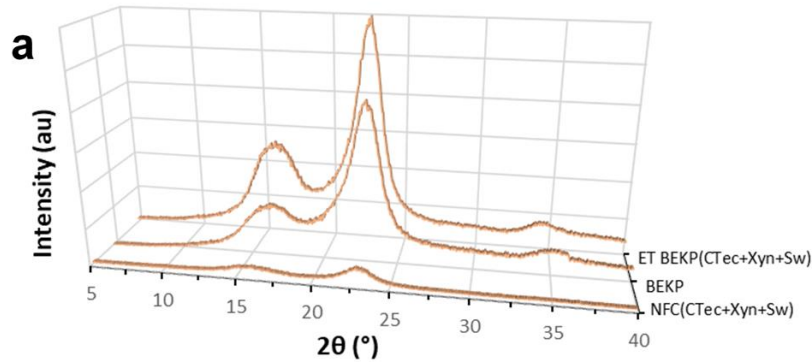
476 3.5. X-ray diffraction

477 X-ray diffraction (XRD) was used in this study to evaluate changes in the relative crystallinity index
478 (CrI) of BEKP until the production of NFC by enzymatic pretreatment since it is widely used to investigate the
479 crystal structure of cellulosic materials (Foster et al., 2018). CrI is based on the Segal method (Segal et al.,
480 1959) which, despite some objections and fault found by other authors (Park et al., 2010; French and Santiago-
481 Cintrón, 2013), it is commonly used to analyse XRD spectra to determine CrI due to its simplicity. XRD curves
482 and CrI of BEKP, enzyme-treated BEKP, and NFC samples are shown in Figure 5. According to Figure 5b, the
483 CrI of BEKP, enzyme-treated BEKP samples, and NFC from BEKP were 68%, 76-79%, and 67-76%,
484 respectively. The CrI of the enzyme-treated BEKP samples resulted higher (12-16% increase) than the CrI of
485 BEKP, which was mainly due to the removal of cellulose disordered regions and amorphous hemicellulose
486 during enzymatic pretreatment. Even though the CrI of the enzyme-treated BEKP samples resulted higher than
487 the CrI of BEKP, differences in the CrI values were observed for the different enzyme-treated samples. These
488 differences may be related to the hemicellulose removal during enzymatic pretreatment under the different
489 conditions evaluated, since it was previously shown that decreasing hemicellulose content in pulps increases
490 crystallinity, possibly by the apparent partial recrystallization of amorphous cellulose regions to crystalline, or
491 partial co-crystallization of crystallites in adjacent fibers (Wan et al., 2010). However, it should be noted that
492 further increasing hemicellulose removal (e.g. by swollenin addition) did not increase CrI of enzyme-treated
493 BEKP. This may be explained by the possible presence of grooves in cellulose structure due to high
494 hemicellulose extensive removal, which was previously shown to result in lower CrI values (Wan et al., 2010).

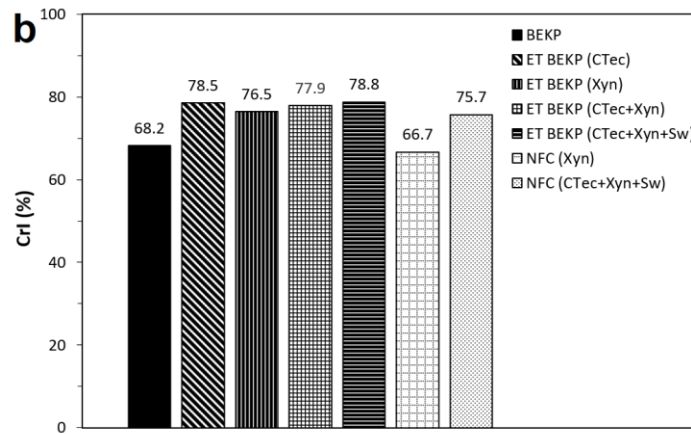
495 On the other hand, XRD measurements showed that NFC obtained after ultrasonication resulted in
496 lower CrI values (67-76%) compared to that of the enzyme-treated BEKP samples. This indicates breakage of
497 the intermolecular hydrogen bonds between cellulose chains during mechanical pretreatment, which caused
498 damage or peeling of the cellulose crystalline structure. This was also observed by Tonoli et al. (2012), who

499 reported a certain degree of damage to the NFC crystalline region when ultrasonication pretreatment was
500 performed.

501



502



503

504 **Fig 5.** (a) XRD pattern and (b) CrI of BEKP, enzyme-treated (ET) BEKP and NFC obtained under different
505 enzymatic pretreatment conditions. CTec, Xyn and Sw are assigned to CTec3, HTec and swollenin,
506 respectively.

507

508 3.6. Thermal analysis

509 Thermal stability of BEKP, enzyme-treated BEKP, and NFC samples was investigated through sample
510 mass change using thermogravimetric analysis (TGA). Figure 6 shows the TGA and derivative
511 thermogravimetric (DTG) curves of the different samples. According to the TGA curves, the material weight
512 loss during sample heating can be divided into three regions of temperature degradation. The first region starts
513 below 150°C and is attributed to water evaporation on the sample's surface. The second region starts above

514 200°C until 300°C and represents the thermal decomposition of hemicelluloses, which result more susceptible
515 to thermal degradation than cellulose and lignin mainly due to the presence of acetyl groups. The third and
516 major weight loss happens at high temperatures (310-390°C) due to cellulose thermal decomposition. Thus, a
517 dominant peak is observed in the DTG curves at maximum weight loss. On the other hand, small portions of
518 lignin in the biomass decompose over a broader degradation temperature range (250-700°C) than cellulose and
519 hemicellulose components due to its aromatic ring structure. Table 3 summarizes the thermal properties of the
520 different samples. The thermal decomposition onset temperature (T_{on}) represents the temperature of the
521 beginning of the degradation, and the maximal weight loss temperature (T_{max}) represents the temperature of the
522 maximum degradation rate. An increase on the T_{on} and T_{max} was observed for the enzyme-treated BEKP samples
523 compared to BEKP, probably due to the removal of amorphous hemicellulose and non-crystalline cellulose
524 regions during enzymatic pretreatment. Among the different enzyme-treated BEKP samples, it can be observed
525 that higher T_{on} values (340-342°C) were obtained for samples with higher xylan release (76-85%) during
526 enzymatic pretreatment, which demonstrates that the removal of non-cellulosic components (e.g. xylan) helps
527 to increase the thermal stability.

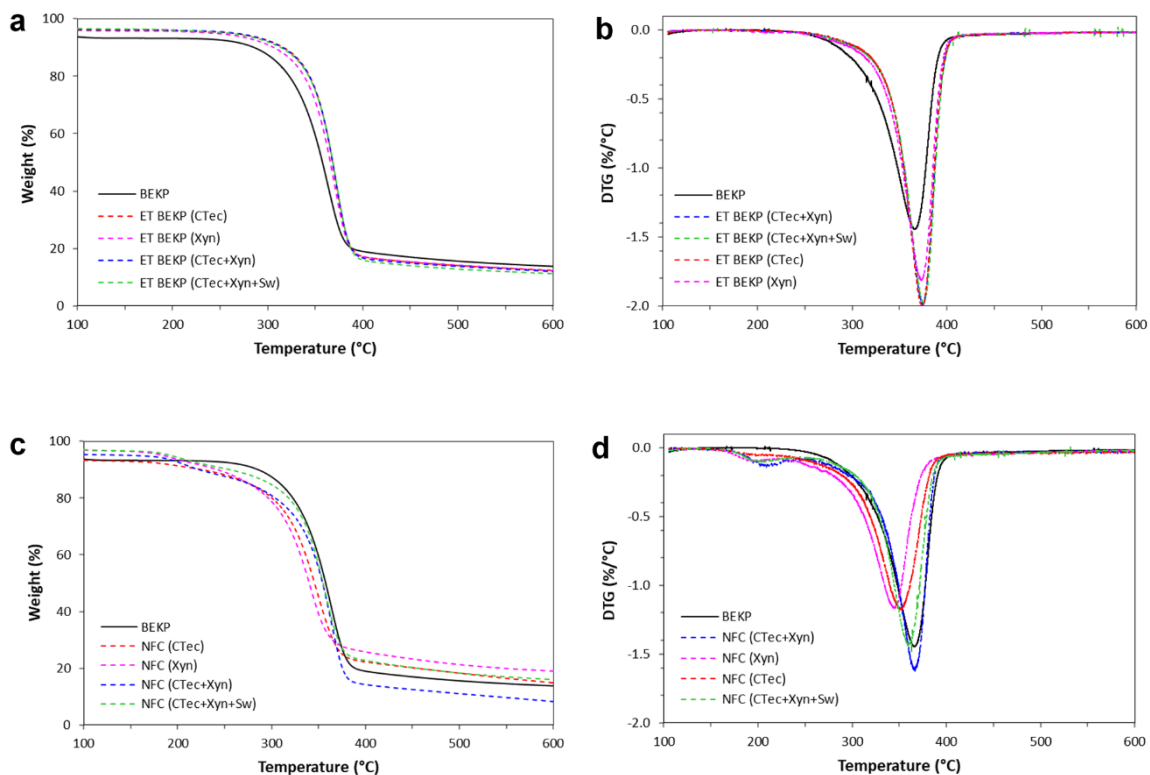
528 On the other hand, the obtained NFC samples had a lower T_{on} and T_{max} , due to damages in cellulose
529 crystalline region that occurred during ultrasonication, as it was already observed by XRD analysis. Moreover,
530 several factors such as size reduction, degree of polymerization decrease, and specific surface area increase that
531 occurred during ultrasonication may decrease the thermal stability of the samples. However, the thermal
532 stability of NFC samples obtained in this study resulted better than that previously reported for NFCs produced
533 by TEMPO-mediation oxidation or acid hydrolysis (Fukuzumi et al. 2010; Lv et al. 2019).

534

535 **Table 3.** Thermal properties of BEKP, enzyme-treated (ET) BEKP and NFC samples.

Sample	T _{on} (°C)	T _{max} (°C)	Residue (%)
BEKP	314	365	13.8
ET BEKP (CTec)	335	374	12.3
ET BEKP (Xyn)	330	372	12.2
ET BEKP (CTec+Xyn)	340	375	12.0
ET BEKP (CTec+Xyn+Sw)	342	375	11.2
NFC (CTec)	300	350	14.9
NFC (Xyn)	292	345	19.0
NFC (CTec+Xyn)	324	368	8.3
NFC (CTec+Xyn+Sw)	320	360	16.0

536



537

538

539 **Fig 6.** (a, c) Thermogravimetric analysis and (b, d) derivative thermogravimetric (DTG) curves of BEKP,
 540 enzyme-treated (ET) BEKP and NFC produced under different enzymatic pretreatment conditions. CTec, Xyn
 541 and Sw are assigned to CTec3, HTec and swollenin, respectively.

542 **4. Conclusions**

543 Enzyme-treated BEKP was effectively fibrillated by ultrasonication. The effects of enzymatic pretreatment
544 on both enzyme-pretreated pulp and NFC properties were investigated. Physicochemical characteristics of
545 enzyme-treated fibers demonstrated that the synergism effect between xylanase enzyme cocktail and swollenin
546 during cellulase pretreatment could greatly open up the eucalyptus pulp fibers by selective removal of
547 hemicellulose and fiber morphology changes, increasing cellulose accessibility without compromising cellulose
548 properties. Thus, relatively high NFC yields were achieved with selective enzyme cocktail mediated
549 pretreatment of cellulose, followed by ultrasonication. The combination of enzymatic and ultrasonication
550 yielded cellulose nanofibers with diameters of 3-10 nm, constituting a potential strategy to isolate nanofibers
551 from different BEKP. Production of NFC from BEKP by the proposed process also affords significant amount
552 of sugars released as a coproduct, which can have further biotechnological applications through the production
553 of value-added chemicals.

554

555 **5. Acknowledgments**

556 Florencia Cebreiros thanks the CAP-UdelaR and ANII from Uruguay for the PhD scholarship and student
557 mobility award (MOV_IDRC_2018_1_151791), respectively. The authors would like to thank UPM Fray
558 Bentos (Uruguay) for providing the raw material, Novozymes (Davis, CA) for providing the enzymes, and VTT
559 Technical Research Center (Finland) for providing the swollenin used in this work. Financial support was
560 provided by Agencia Nacional de Investigación e Innovación (ANII_FMV_1_2019_1_156233, Uruguay).

561

562 **6. References**

563 Abdul Khalil HPS, Davoudpour Y, Nazrul Islam Md, Mustapha A, Sudesh K, Dungani R, Jawaaid M (2014)
564 Production and modification of nanofibrillated cellulose using various mechanical processes: a review.
565 Carbohydr Polym 99:649-665.
566 Abitbol T, Rivkin A, Cao Y, Nevo Y, Abrahan E, Ben-Shalom T, Lapidot S, Shoseyov O (2016) Nanocellulose,
567 a tiny fiber with huge applications. Curr Opin in Biotech 39:76-88.

568 Adsul M, Sandhu SK, Singhania RR, Gupta R, Puri SK, Mathur A (2020) Designing a cellulolytic enzyme
569 cocktail for the efficient and economical conversion of lignocellulosic biomass to biofuels. *Enzyme Microb*
570 *Tech* 133:109442.

571 Aïssa K, Karaaslan MA, Renneckar S, Saddler JN (2019) Functionalizing cellulose nanocrystals with click
572 modifiable carbohydrate-binding modules. *Biomacromolecules* 20(8):3087-3093.

573 Arantes V, Dias IKR, Berto GL, Pereira B, Marotti BS, Nogueira CFO (2020) The current status of the enzyme-
574 mediated isolation and functionalization of nanocelluloses: production, properties, techno-economics, and
575 opportunities. *Cellulose* (2020). <https://doi.org/10.1007/s10570-020-03332-1>.

576 Baati R, Magnin A, Boufi S (2017) High solid content production of nanofibrillar cellulose via continuous
577 extrusion. *ACS Sustain Chem Eng* 5:2350-2359.

578 Bondancia TJ, Mattoso LHC, Marconcini JM, Farinas CS (2017) A new approach to obtain cellulose
579 nanocrystals and ethanol from eucalyptus cellulose pulp via the biochemical pathway. *Biotechnol Prog*
580 33:1085-1095

581 Chandra R, Ewanick S, Hsieh C, Saddler JN (2008) The characterization of pretreated lignocellulosic substrates
582 prior to enzymatic hydrolysis, part 1: a modified simons' staining technique. *Biotechnol Prog* 24:1178–
583 1185.

584 Debiagi F, Faria-Tischer PCS, Mali S (2020) Nanofibrillated cellulose obtained from soybean hull using simple
585 and eco-friendly processes based on reactive extrusion. *Cellulose* 27:1975–1988.

586 De Campos A, Correa AC, Cannella D, Teixeira EM, Marconcini JM, Dufresne A, Mattoso LHC, Cassland P,
587 Sanadi AR (2013) Obtaining nanofibers from curauá and sugarcane bagasse fibers using enzymatic
588 hydrolysis followed by sonication. *Cellulose* 20:1491–1500.

589 Di Giorgio L, Salgado PR, Dufresne A, Mauri AN (2020) Nanocelluloses from phormium (*Phormium tenax*)
590 fibers. *Cellulose* 27:4975–4990.

591 Djafari Petroudy SR, Ghasemian A, Resalati H, Syverud K, Chinga-Carrasco G (2015) The effect of xylan on
592 the fibrillation efficiency of DED bleached soda bagasse pulp and on nanopaper
593 characteristics. *Cellulose* 22:385–395.

594 Ferreira RR, Souza, AG, Nunes, LL, Shahi N, Rangari VK, dos Santos Rosa D (2020) Use of ball mill to prepare
595 nanocellulose from eucalyptus biomass: Challenges and process optimization by combined method. *Mater*
596 *Today Commun* 22:100755.

597 Filson PB, Dawson-Andoh BE, Schwegler-Berry D (2009) Enzymatic-mediated production of cellulose
598 nanocrystals from recycled pulp. *Green Chem* 11:1808-1814.

599 Foster EJ, Moon RJ, Agarwal UP, Bortner MJ, Bras J, Camarero-Espinosa S, Chan KJ, Clift MJD, Cranston
600 ED, Eichhonor SJ, Fox DM, Hamad WY, Heux L, Jean B, Korey M, Nieh W, Ong KJ, Reid MS, Renneckar
601 S, Roberts R, Shatkin JA, Simonsen J, Stinson-Bagby K, Wanasekara N, Youngblood J (2018) Current
602 characterization methods for cellulose nanomaterials. *Chem Soc Rev* 47:2511-3006.

603 French AD, Santiago-Cintrón M (2013) Cellulose polymorphy, crystallite size, and the Segal Crystallinity
604 Index. *Cellulose* 20:583-588.

605 Fukuzumi H, Saito T, Okita Y, Isogai A (2010) Thermal stabilization of TEMPO-oxidized cellulose. *Polym*
606 *Degrad Stabil* 95:1502-1508.

607 Gomes VJ, Longue D, Colodette JL, Ribeiro RA (2014) The effect of eucalypt pulp xylan content on its
608 bleachability, refinability and drainability. *Cellulose* 21:607-614.

609 Gourlay K, Arantes V, Saddler JN (2012) Use of substructure-specific carbohydrate binding modules to track
610 changes in cellulose accessibility and surface morphology during the amorphogenesis step of enzymatic
611 hydrolysis. *Biotechnol Biofuels* 5:51.

612 Gourlay K, Hu J, Arantes V, Andberg M, Saloheimo M, Penttilä M, Saddler J (2013) Swollenin aids in the
613 amorphogenesis step during the enzymatic hydrolysis of pretreated biomass. *Bioresour Technol* 142:498-
614 503.

615 Hamad WY, Hu TQ (2010) Structure-process-yield interrelations in nanocrystalline cellulose extraction. *Can J*
616 *Chem Eng* 88:392-402.

617 Hu J, Arantes V, Saddler JN (2011) The enhancement of enzymatic hydrolysis of lignocellulosic substrates by
618 the addition of accessory enzymes such as xylanase: is it an additive or synergistic effect? *Biotechnol*
619 *Biofuels* 4:36.

620 Hu J, Tian D, Renneckar S, Saddler JN (2018) Enzyme mediated nanofibrillation of cellulose by the synergistic
621 actions of an endoglucanase, lytic polysaccharide monoxygenase (LPMO) and xylanase. *Sci Rep* 8:3195.

622 Immergut EH, Schurz J, Mark H (1953) Viscosity-number-molecular weight relationship for cellulose and
623 investigations of nitrocellulose in various solvents. *Monatsh Chem* 84:219–249.

624 Qua EH, Hornsby PR, Sharma HSS, Lyons G (2011) Preparation and characterization of cellulose nanofibers.
625 *J Mater Sci* 46:6029-6045.

626 Long L, Tian D, Hu J, Wang F, Saddler J (2017) A xylanase-aided enzymatic pretreatment facilitates cellulose
627 nanofibrillation. *Bioresour Technol* 243:898-904.

628 Lv D, Du H, Che X, Wu M, Zhang Y, Liu C, Nie S, Zhang X, Li B (2019) Tailored and integrated production
629 of functional cellulose nanocrystals and cellulose nanofibrils via sustainable formic acid hydrolysis: kinetic
630 study and characterization. *ACS Sustain Chem Eng* 7:8827-8833.

631 Mahardika M, Abral H, Kasim A, Arief S, Asrofi M (2018) Production of nanocellulose from pineapple leaf
632 fibers via high-shear homogenization and ultrasonication. *Fibers* 6:28.

633 Merklein K, Fong SS, Deng Y (2016) Chapter 11-Biomass utilization. In: Eckert C and Trinh C (ed)
634 *Biotechnology for Biofuel Production and Optimization*, 1st Edition. Elsevier, pp 291-324

635 Michelin M, Gomes D, Romaní A, Polizeli MLTM, Teixeira JA (2020) Nanocellulose Production: Exploring
636 the Enzymatic Route and Residues of Pulp and Paper Industry. *Molecules* 25:3411.

637 Morrison JM, Elshahed MS, Youssef NH (2016) Defined enzyme cocktail from the anaerobic fungus
638 *Orpinomyces* sp. Strain C1A effectively releases sugars from pretreated corn stover and switchgrass. *Sci*
639 *Rep* 6:29217.

640 Park S, Baker JO, Himmel ME, Parilla PA, Johnson DK (2010) Cellulose crystallinity index: measurement
641 techniques and their impact on interpreting cellulase performance. *Biotechnol Biofuels* 3:1-10.

642 Pereira B, Arantes V (2020) Production of cellulose nanocrystals integrated into a biochemical sugar platform
643 process via enzymatic hydrolysis at high solid loading. *Ind Crop Prod* 152:112377.

644 Pires JRA, Souza VGL, Fernando AL (2019) Valorization of energy crops as a source for nanocellulose
645 production – Current knowledge and future prospects. *Ind Crop Prod* 140:111642.

646 Phanthong P, Reubroycharoen P, Hao X, Xu G, Abudula A, Guan G (2018) Nanocellulose: Extraction and
647 application. *Carbon Resour Convers* 1:32-43.

648 Rajinipriya M, Nagalakshmaiah M, Robert M, Elkoun S (2018) Importance of agricultural and industrial waste
649 in the field of nanocellulose and recent industrial developments of wood based nanocellulose: a review.
650 ACS Sustain Chem Eng 6:2807-2828.

651 Ramakrishnan A, Ravishankar K, Dhamodharan R (2019) Preparation of nanofibrillated cellulose and
652 nanocrystalline cellulose from surgical cotton and cellulose pulp in hot-glycerol medium. Cellulose
653 26:3127-3141.

654 Reese ET, Segal L, Tripp VW (1957) The effect of cellulase on the degree of polymerization of cellulose and
655 hydrocellulose. Text Res J 27:626-632.

656 Ribeiro RSS, Pohlmann BC, Calado V, Bojorge N, Pereira Jr N (2019) Production of nanocellulose by
657 enzymatic hydrolysis: trends and challenges. Eng Life Sci 19:279-291.

658 Saloheimo M, Paloheimo M, Hakola S, Pere J, Swanson B, Nyssönen E, Bhatia A, Ward M, Penttilä M (2002)
659 Swollenin, a *Trichoderma reesei* protein with sequence similarity to the plant expansins, exhibits disruption
660 activity on cellulosic materials. Eur J Biochem 269:4202-4211.

661 Segal L, Creely JJ, Martin AE, Conrad CM (1959) An empirical method for estimating the degree of
662 crystallinity of native cellulose using the X-ray diffractometer. Text Res J 29:786-794.

663 Tibolla H, Pelissari FM, Martins JT, Vicente AA, Menegalli FC (2018) Cellulose nanofibers produced from
664 banana peel by chemical and mechanical treatments: Characterization and cytotoxicity assessment. Food
665 Hydrocoll 75:192-201.

666 Tonoli GHD, Teixeira EM, Corrêa AC, Marconcini JM, Caixeta LA, Pereira-da-Silva MA, Mattoso LHC
667 (2012) Cellulose micro/nanofibers from *Eucalyptus* kraft pulp: preparation and properties. Carbohydr
668 Polym 89:80-88.

669 Tsukamoto J, Durán N, Tasic L (2013) Nanocellulose and bioethanol production from Orange waste using
670 isolated microorganisms. J Brazil Chem Soc 24:1537-1543.

671 Wan J, Wang Y, Xiao Q (2010) Effects of hemicellulose removal on cellulose fiber structure and recycling
672 characteristics of eucalyptus pulp. Bioresour Technol 101:4577-4583.

673 Wang S, Cheng Q (2009) A novel process to isolate fibrils from cellulose fibers by high-intensity
674 ultrasonication, part 1: process optimization. J Appl Polym Sci 113:1270-1275.

675 Wang W, Mozuch MD, Sabo RC, Kersten P, Zhu JY, Jin Y (2014) Production of cellulose nanofibrils from
676 bleached eucalyptus fibers by hyperthermostable endoglucanase treatment and subsequent
677 microfluidization. *Cellulose* 22:351-361.

678 Yadav C, Saini A, Maji PK (2017) Energy efficient facile extraction process of cellulose nanofibers and their
679 dimensional characterization using light scattering techniques. *Carbohydr Polym* 165:276-284.

680 Yarbrough JM, Zhang R, Mittal A, Wall, TV, Bomble YJ, Decker SR, Himmel ME, Ciesielski PN (2017)
681 Multifunctional cellulolytic enzymes outperform processive fungal cellulases coproduction of nanocellulose
682 and biofuels. *ACS Nano* 11:3101-3109.

683 Zhou H, St. John F, Zhu JY (2019) Xylanase pretreatment of wood fibers for producing cellulose nanofibrils:
684 a comparison of different enzyme preparations. *Cellulose* 26:543–555.

685